Article

Chemical Recycling of Plastic Marine Litter: First Analytical Characterization of The Pyrolysis Oil and of Its Fractions and Comparison with a Commercial Marine Gasoil

Gian Claudio Faussone [1,2,*] and Teresa Cecchi [3,*]

1   Sintol, Corso Matteotti 32A, 10121 Torino, Italy
2   University of Nova Gorica, Vipavska 13, SI-5000 Nova Gorica, Slovenia
3   ITT Montani, Via Montani 7, 63900 Fermo, FM, Italy
*   Correspondence: gianclaudio@sintol.it (G.C.F.); cecchi.teresa@istitutomontani.edu.it (T.C.);
    Tel.: +39-0117790061 (G.C.F.); +39-0734-622632 (T.C.)

Abstract: A detailed molecular fingerprint of raw pyrolysis oil from plastic wastes is a new research area. The present study focuses for the first time on the chemical recycling of plastic marine litter; we aim to chemically characterize the obtained raw pyrolysis oil and its distillates (virgin naphtha and marine gasoil) via GC-MS and FT-IR. For all samples, more than 30% of the detected compounds were identified. 2,4-dimethyl-1-heptene, a marker of PP pyrolysis, is the most represented peak in the chemical signature of all the marine litter pyrolysis samples, and it differentiates commercial and pyrolysis marine gasoil. The presence of naphthalenes is stronger in commercial gasoil, compared to its pyrolysis analog, while the opposite holds for olefins. The overlap between the two molecular fingerprints is impressive, even if saturated hydrocarbons are more common in commercial gasoil, and unsaturated compounds are more common in the gasoil derived from pyrolysis. A technical comparison between the commercial marine gasoil and the one obtained from the marine litter pyrolysis is also attempted. Gasoil derived from marine litter fully complies with the ISO8217 standards for distillate marine fuel. On the other hand, the virgin naphtha is particularly rich in BTX, ethylbenzene, styrene, and alpha olefins, which are all important recoverable platform chemicals for industrial upcycling.

Keywords: virgin naphtha; marine gasoil; pyrolysis marker; ISO8217; BTX; platform chemicals; marine litter

1. Introduction

Plastic waste is a long-lasting and worldwide ecological problem. Plastic has become the emblem of waste (disposable objects), pollution, and ecotoxicity. It is estimated that in 2018, an estimated 14.5 million tons of plastics entered the ocean [1], building up each year a stock of plastic waste undergoing progressive fragmentation and releasing microparticles that enter the food chain with unknown consequences. Personal protective and single-use products associated with the current COVID-19 pandemic will probably increase the quantities of plastic entering the oceans [2]. Landfilling, incineration with or without energy recovery, and recycling are common ways to manage plastic waste. However, safe landfilling is expensive and does not fit the sustainable circular economy vision; incineration may lead to the emission of harmful greenhouse gases (NOx, SOx, COx, etc.) and other toxic volatiles. Noteworthy is that not all plastics can be mechanically recycled, considering their degradation states, complex compositions, or mixtures with other substances [3]; and sorting mixed plastic waste is a labor intensive and expensive prerequisite of the process since most plastics are not compatible with each other and can't be processed together during recycling [4]. This is particularly true for plastic marine litter, which is mainly landfilled or incinerated [5].

In this context, chemical recycling, specifically pyrolysis, provides a promising way to upcycle plastic wastes, and it can be used to produce fuels or important chemical building blocks for the petrochemical industry. The main advantage of the pyrolysis process over the mechanical recycling process is the fact that it does not need sorting and cleaning steps, at least to a great extent, which is obviously beneficial to treat difficult feedstocks, such as plastic marine litter, which is often collected as "bycatch" by fishermen and must be separated from the catch with loss of time and additional work. The pyrolysis of plastic generates a gas fraction, a liquid fraction (pyrolysis oil), which is composed of several hydrocarbon species (depending on process conditions and plastic type), and solid residues, [6,7]. The economics of the process is interesting because the production cost of pyrolysis fuel is ca. 10 times lower than the market fuel prices in the case of a 10,000 kg/h plant [8]; and in the case of marine litter, the conversion into "drop in" fuels can become an effective nonmonetary reward for the depollution of the ocean. Another important motivation for producing pyrolysis oil from waste plastic is an overall reduction of about 30% in NOx, CO, and HC emissions observed in comparison with neat diesel [9]. Even if the circular economy approach to plastic waste management does not fully endorse chemical recycling, since produced fuels are just energy carriers, there are at least three cases in which the latter approach is the best strategy: (i) nonrecycled plastics, defined as the rejected streams (unable to be processed due to certain restrictions) that remain in the mechanical recycling centers, (ii) hospital plastics that might involve a severe biohazard, and (iii) highly nonhomogeneous and contaminated plastic waste, such as marine litter, which also comprises a wide array of other nonplastic materials, such as biomass, sand, clothes, glass, metals, etc.

Besides, the light distillate of pyrolysis oil can become the feedstock for the synthesis of second-generation raw polymers using existing technologies, such as steam cracking, thus providing a new perspective about the potential of chemical recycling to deliver second-generation raw materials and hence its full integration within the circular economy concept [4,10].

Pyrolysis oil and its distillates were often characterized as regards their physical–chemical properties and compliance with ASTM and ISO standards; their chemical composition was analyzed via GC-MS, the most eligible technique, due to the volatile nature of the compounds and/or their possible volatilization in the heated injection port of the gas-chromatograph. However, in many studies, the absence of a scrupulous description of the sampling procedure prevents any comment on the experimental outcomes since the preanalytical step strongly influences the results; light compounds are often missing probably because the solvent used to prepare the oil solutions to be injected interferes with the detection of the most volatile compounds.

The pyrolysis oils that were tested via GC-MS were usually obtained from specific kinds of plastics [11–14] or their partial mixture [15], and a meticulous molecular description of the samples was usually omitted. In this respect, common model plastics were PS [16–18]; PET, HDPE, LDPE, PP, PS, and PVC [11]; HDPE, LDPE, PP, and PS [19]; PE [20,21]; LDPE and HDPE [22]; LDPE, the mixture of HDPE and LDPE, PP, and HDPE [23]; PP [24]; and PP and LDPE [25]. The complete chemical fingerprint of the pyrolysis oil from mixed plastic waste was rarely studied, and only a few compounds were usually identified in their pyrolysis oils, while analytes were usually not detailed since they were grouped according to specific criteria, such as the carbon number or chemical class [26]. Only very few studies provided the complete molecular description of pyrolysis oils from mixed plastic waste: Lopez et al. studied the pyrolysis oil from rejected streams that was unable to be processed due to restrictions, which come from industrial plants where plastic wastes are classified and separated for their subsequent mechanical recycling. They found that the end product was a complex mixture of organic compounds containing more than 70% of valuable chemicals (styrene, toluene, ethyl-benzene, and alpha-methylstyrene); branched alkanes and alkenes were missing [14]. Cho et al. focused on BTX and other aromatics yield

from the pyrolysis of mixed plastic waste from a recycling facility; aliphatic compounds were not detailed. The reaction temperature had a positive effect on the BTX yield [27].

A high resemblance of pyrolysis oil from municipal plastic waste with standard diesel was demonstrated on the basis of thorough GC-MS analyses, even if the sampling conditions were not detailed, and compounds lighter than C8 alkanes and C7 aromatics were not detected [28].

From the review of the literature, it follows that, to date, only a few studies describe a detailed molecular fingerprint of pyrolysis oil from plastics wastes, and just two studies deal also with the characterization of its distillates. Singh et al. indicated 13 major compounds in pyrolysis oil from mixed plastics and compared its composition to that of HDPE, PP, and PS pyrolysis oil; the most abundant hydrocarbon fraction in pyrolysis oil based on carbon number is the C5-C12 fraction. The distilled fraction with a boiling point up to 240 °C was found to contain 13.85% 2,4-dimethyl-1-heptene, 8.67% 1,1,3,4-tetramethyl cyclopentane, 4.35% 2-Octen-4-one, 4.27% 1,3,5-trimethyl cyclohexane, and higher quantity of the C9 and C10 compounds and branched alkanes and alkenes [29]. The rejected fraction of the packaging waste was pyrolyzed. GC-MS results for the pyrolysis oil and its distillate revealed high levels of aromatics (recoverable building blocks for industrial use), alkanes, cycloalkanes, alkenes, cycloalkenes, and oxygenated compounds for a total of 33 analytes. However, the authors did not describe how the samples were processed. Styrene was the principal aromatic compound, followed by ethylbenzene and toluene [3].

Noteworthy is that no investigation (neither exhaustive nor general) on the chemical composition of the raw pyrolysis oil (and its distillates) from marine litter is available in the scientific literature.

Taking into account this scarcity of available data and the fact that pyrolysis oil from plastic waste can lead to alternative fuels and valuable chemicals for a more sustainable industry, we believe that it is crucial to provide the detailed chemical composition and obtain a molecular fingerprint of the fuels that can be obtained via the chemical recycling of the marine litter for both scientific and commercial reasons. In the following, we describe the pyrolysis process of the marine litter and its characterization, especially at the molecular level via the GC-MS analysis of the raw pyrolysis oil (RPO ml-py) and its distilled fractions, namely, virgin naphtha (VN ml-py) and marine gasoil (MGO ml-py). The FTIR analysis provides an additional chemical signature of the samples. A comparison between the molecular signature of the MGO obtained from marine litter pyrolysis and the commercial MGO is also carried out along with their physicochemical characterization. This comparison may pave the way to the removal of regulatory barriers within a chemical recycling regulatory framework.

2. Materials and Methods

2.1. Plastic Wastes Feedstock

Within the EU project "Mapping and recycling of marine litter and Ghost nets on the sea floor" (marGnet), more than 200 kg of actual plastic marine litter was collected from the sea bottom of the Venice Lagoon and north Adriatic Sea by scuba divers with the goal to pyrolyze it "as it is" without any sorting or pretreatment and upgrade the pyrolysis oil to ISO-compliant marine fuel by means of distillation. The focus on sunk litter is justified because it is estimated that as much as 70% of marine debris sinks to the seabed, and even low-density polymers can lose buoyancy under the weight of fouling [30]. Although a precise characterization of the plastic litter was not possible due to the high amount of dirt and organic incrustation or the lack of identifying markings, two thirds of the collected plastic litter were general plastic containers, such as hard boxes and packaging films, plastic bottles, plastic nets from mussel farming, and a few boat components, and one third was fishing nets. This is confirmed in literature where it is reported that plastic items, bags, and fishing equipment are the largest part of the debris at sea [31], and benthic marine litter in the central Mediterranean Sea is composed of 68% general plastic objects and 32% fishing gear [32]. A small contribution of floating litter mainly composed of styrofoam and floating

containers was also included in the feedstock. The great majority of postconsumer plastic waste is made from just three polymer families: PE, PP, and PET [33], while the fishing nets are mainly made of nylons (6 and 6.6) and PE, and mussel nets are made of PP, we can assume that the composition of the plastic marine litter was essentially made of polyolefins and polyamides with contributions of polystyrene and rubber. Organic matter, such as seaweed, mussel residue, etc., was the main recognizable contaminant along with sand. Nonplastic items easily recognizable, such as glass bottles and metals cages, were manually segregated and removed during collection. Scrap tires were also present as litter in the sea, but their pyrolysis products are not discussed in this work.

2.2. Pyrolysis Process

For the pyrolysis experiments, a cylindrical 100 L volume reactor, heat insulated, AISI 304 stainless steel, internal diameter 320 mm, 1:3 diameter to height ratio, electrically heated was employed (provider SINTOL, Torino, Italy). The reactor wall was maintained at 400 +/− 50 °C temperature and autogenic pressure by electric heaters (total rated power 15 KW). A shell and tube AISI 304 stainless steel 0.42 m^2 condenser, water-cooled, located just at the outlet of the pyrolysis reactor collected the vapors of RPO (ml-py) in a receiving tank. Noncondensable gas was flared after conditioning. The operation was batchwise, and 14 pyrolysis cycles performed with loads of dry plastic marine litter ranging from a minimum of 4 kg to a maximum of 11.5 kg for a total of 100 kg. Each pyrolysis cycle lasted 4 h from start to end. Pyrolysis oil collected from each cycle was homogenized in order to provide the overall mean composition. After every pyrolysis cycle, the reactor was cleaned and solid residues were removed. A total of 1 kg of calcium oxide-based additive (content of CaO > 57 wt%; CaO + MgO > 92 wt%; CalcePiasco, Italy) was added to the feedstock in the reactor for each cycle to avoid the formation of acidic compounds, such as hydrochloric acid and other organic acids, as also described elsewhere [34]. Mass balance was 45 wt% RPO (ml-py), 26 wt% noncondensed gas, and 26 wt% solid residues (net of additive).

2.3. Pyrolysis Oil Distillation

Simple distillation of the RPO (ml-py) was performed with a 50 L AISI 304 stainless steel distillation flask. The first cut temperature was 180 °C collecting the light fraction, namely the VN (ml-py); the second cut temperature was set to 320 °C collecting the targeted product, namely, the MGO (ml-py). Residual product distilling above 320 °C was recovered as residue from the distillation flask. Since simple distillation cannot guarantee sharp splits, some degree of overlapping components in the distillates was expected. Mass balance was 23 vol% VN (ml-py), 52 vol% MGO (ml-py), 6 vol% residue, 10 vol% water, and 9 vol% loss as gas due to cracking reactions.

MGO (my-pl) was filtered with silica gel granules (diameter 0.5 mm, porosity 800 m^2/g, provider Bolaseca, Murcia, Spain) to remove residual humidity and give it a clearer appearance.

2.4. GC–MS Analysis

The RPO (ml-py) and its distilled fractions, namely, VN (ml-py), MGO (ml-py), and MGO (comm), were characterized by gas chromatography to detail their chemical composition and properties. Three replicate samples were used for the chromatographic analysis. A Hewlett Packard GC-MS, G1800C GCD Series II (Palo Alto, Santa Clara, CA, USA), equipped- with an HP-5MS column 30 m × 0.25 mmI.D. × 0.25 μm film thickness (Hewlett-Packard) was used. The mass spectrometer was tuned before the analyses via a reference gas (perfluorotributylamine) across the full mass range. The injector was set at 325 °C and operated in the split mode (split ratio 1:240). The carrier gas was helium with a constant flow of 1 mL/min; the oven temperature was held isothermal at 30 °C for 15 min, then programmed from 30 °C to 100 °C at 5 °C/min, and then programmed from 100 °C to 325 °C at 10 °C/min and held isothermal at 325 °C for 10 min. Mass spectra were acquired in the electron impact mode (70 eV), using a full scan with mass analysis in the range 10 atomic mass units (amu)–450 atomic mass units (amu). The ion source and the quadrupole were

heated by conduction. A total of 2.500 mL of each sample were filtered to remove organic materials larger than 5 µm and put in 5 mL headspace vial, closed by PTFE/silicone septum. Both the liquid phase and the volatiles in the headspace of the samples were analyzed, respectively, via the direct injection of 1 µl of the liquid in the injection port of the GC-MS and HS-SPME-GC-MS. SPME fibers were obtained from the Supelco Company (Bellefonte, PA, USA). The fiber (divinylbenzene/carboxen/polydimethylsiloxane 50/30 µm) was selected because it is considered the most universal [35–38]; it was conditioned before use, as recommended by the manufacturer. Before extraction, the stabilization of the headspace in the vial was reached by equilibration for 30 min at 30 °C ± 0.1 °C. Volatiles were then adsorbed for exactly 10 h at 30 °C ± 0.1 °C. After extraction, injections provided the fiber thermal desorption into the GC-MS injection port equipped with a 0.75 mm i.d. inlet liner. Before the subsequent sampling, the fiber was reconditioned for 5 min at 325 °C. Blank runs (empty injections) were done periodically during the study to reveal possible carryover. Carryover never occurred.

The identification of the analytes was based on the comparison of their retention times with those of standards obtained from Sigma-Aldrich (Milan, Italy). The purity of the volatile standards was usually 97% or higher. In the absence of a commercial standard, peak identification was carried out by (i) computer matching of mass spectral data with those of compounds contained in the Mass Spectral Library of the National Institute of Standards and Technology (NIST 1998 library); the quality of the match above 98% was needed for positive identification; (ii) comparison of their linear retention indices [37,39] relative to n-alkanes, calculated using a straight-chain alkane mixture, with the averaged values reported in the bibliography for chromatographic columns similar to that used. Only compounds with a signal-to-noise ratio higher than 5 were considered. The relative proportions of the constituents in the samples were obtained using the percentage area of chromatographic peaks, as usual [35–39]. The statistical analysis of the variance was performed via the data analysis tool in Microsoft ® Excel for Mac, version 16.16.26 (200914) © 2022 Microsoft.

2.5. Fourier Transform Infrared (FTIR) Spectroscopy

The pyrolysis oil, its distillates, and a commercial MGO were analyzed via FTIR (PerkinElmer; Model: Spectrum II) in the wave range of 4000–600 cm^{-1} via the UATR arrangement to identify functional groups.

2.6. ISO8217:2017 Analysis

The MGO (ml-py) was analyzed as per compliance with ISO8217:2017, DMA/DMX, distillate fuel classification. Therefore, all parameters were evaluated according to the ISO 8217:2017 prescribed standard methods for marine fuels (ISO, 2017), except for oxidation stability that was determined by the DIN EN 16091:2012 method.

3. Results and Discussion

3.1. ISO Compliance of MGO (ml-py)

The marGnet project had the general goal to tackle marine litter from a multilevel approach with a specific focus on what to do with marine litter once recovered from the sea [40]. The answer was to convert marine litter into marine fuels, being a sort of payback for fishermen and other stakeholders involved in the collection activity. Giving back the fuel obtained from the litter the fishermen delivered was a great nonmonetary instrument to attain greater involvement of stakeholders and thus an efficient sea clean up. However, to do so, the produced fuel must be fully compatible with commercial marine gasoil so that no technical issue could arise upon its usage. Compliance with conventional fuel is also crucial to avoid skepticism among stakeholders. Therefore, among the marine fuels classified according to ISO 8217, the highest quality ones, DMX and DMA, were targeted. DMX and DMA are normally commercially referred to MGO.

Table 1 summarizes the analytical values juxtaposed to the prescribed limits for DMX/DMA classification.

Table 1. Analytical results for MGO (ml-py) (excerpt from [41]).

Parameter	Result	Limit	Unit
Kin. Viscosity (50 °C)	1.848	Min. 1.4; max. 6	mm^2/s
Density (15 °C)	802.9	Max. 890	kg/m^3
Cetane index	61.3	Min. 40	-
10% (*V/V*) recovery	178.3	-	°C
50% (*V/V*) recovery	257.1	-	°C
90% (*V/V*) recovery	347.0	-	°C
Sulfur content	196	Max. 1000	ppm
Flash point	58.0	Min. 43	°C
Hydrogen sulfide	<2	Max. 2	ppm
Acid value	0.136	Max. 0.5	mg KOH/g
Sediment content	0.02	-	% (m/m)
Carbon residue	<0.10	Max. 0.3	% (m/m)
Pour point (winter quality)	−6	Max. −6	°C
Pour point (summer quality)	−6	Max. 0	°C
Water content	0.01	-	% (*V/V*)
Ash content (775 °C)	<0.001	Max. 0.01	% (m/m)
Cloud point	14		°C
HFRR (Lubricity at 60 °C)	240	Max. 520	µm
Oxidation stability	15.46	-	min

Table 1 confirms that MGO (ml-py) is compliant with ISO 8217, and therefore this fuel can be used both pure and blended with MGO (comm) in existing engines without any technical modification or adjustment. MGO (comm) is assumed to be compliant with ISO 8217. Noteworthy is the pour point value of −6 °C, which permits the MGO (ml-py) to meet both winter and summer quality requirements, and the sulfur content which is approximately 80% lower than the prescribed value, making the MGO (ml-py) also compliant with the latest requirements of the Emission Control Areas (ECAs) [42]. This is a remarkable result if we consider that MGO (ml-py) was obtained from marine litter once polluting the Adriatic Sea.

Figure 1 shows the visual appearance of the VN (ml-py), MGO (ml-py), and RPO (ml-py) samples.

Figure 1. RPO (**left**), MGO (**middle**), and VN (**right**) samples.

3.2. GC-MS Analysis of the Liquid Samples

The composition of VN (ml-py), MGO (ml-py), and RPO (ml-py), along with the composition of MGO (comm) are shown in Table 2, where the percent areas of all the identified compounds (organized by chromatographic retention) are summarized, and different colors are used for the average percent area below 1% (red), between 1% and 4% (green), and above 4% (yellow). Standard deviations were always below 10%.

Table 2. Literature and calculated retention indexes (RIlit, RIcalc), CAS number, and average percent area (triplicate injections) of analytes from MGO (comm), VN (ml-py), MGO (ml-py), and RPO (ml-py) samples. Different colors are used for average percent area below 1% (red), between 1% and 4% (green), and above 4% (yellow). Standard deviations were always below 10%.

Analyte	Analyte Code	RI Lit	RI Calc	CAS	Average % Area MGO (comm)	Average % Area VN (ml-py)	Average % Area MGO (ml-py)	Average % Area RPO (ml-py)
1-propene-2-methyl		394	399	115-11-7		0.04	0.05	0.14
2-methylbutane	C5	474	480	78-78-4	0.02			
1-pentene	C5	478	483	109-67-1				0.11
pentane	C5	500	499	109-66-0	0.03	1.14	0.16	0.37
2-methyl-1,3-butanediene (isoprene)	C5	520	515	78-79-5		0.11	0.18	0.12
2-methyl-2-butene	C5	525	520	513-35-9		0.12		0.1
1,3-pentadiene	C5	542	538	504-60-9				0.04
1,3-Cyclopentadiene	C5	540	542	542-92-7				0.04
cyclopentene	C5	552	556	142-29-0		0.14		0.06
2-methylpentane	C6	560	563	107-83-5	0.06	0.98	0.06	0.17
3-methylpentane	C6	580	580	96-14-0		0.05	0.07	0.04
1-hexene	C6	588	588	592-41-6	0.11	2.87	0.45	0.87
hexane	C6	600	599	110-54-3	0.04	0.72	0.13	0.32
2-methyl-2-pentene,	C6	606	602	625-27-4	0.03	0.64	0.1	0.22
3-methylcyclopentene	C6	612	612	592-48-3		0.09		0.03
2-hexene, (Z)-	C6	617	615	7688-21-3		0.12		0.05
3-methyl-2-pentene, (E)-	C6	620	621	616-12-6		0.06		0.03
methylcyclopentane	C6	627	628	96-37-7	0.04	0.31		0.11
2,4-hexadiene, (E,Z)-	C6	636	637	5194-50-3		0.2		0.09
3-methyl-1,3-Pentadiene, (Z)	C6	640	642	2787-45-3	0.03	0.23	0.05	0.07
2,4-dimethyl-1-pentene	C7	642	646	2213-32-3		0.82	0.06	0.11
1-methylcyclopentene	C6	647	648	693-89-0		0.39	0.04	0.15
benzene	Benz	663	663	71-43-2	0.05	0.7	0.25	1.08
2-methylhexane	C7	667	667	591-76-4	0.04	0.17		
3-methylhexane	C7	677	676	589-34-4	0.03	0.13		0.03
cyclohexene	C6	678	680	110-83-8		0.28	0.05	0.1
2-methyl-1-hexene	C7	683	688	6094-02-6		0.33	0.22	0.09
1-heptene	C7	692	692	592-76-7	0.09	1.99	0.16	0.64
heptane	C7	700	702	142-82-5	0.13	1.8	0.34	0.59
2-methyl-2-hexene	C7	702	705	2738-19-4		0.51	0.1	0.14
2-heptene, (E)-	C7	705	707	7642-10-6		0.23	0.05	0.09
2-heptene, (z)-	C7	714	716	592-77-8		0.13	0.04	0.07
3-methylcyclohexene	C7	728	726	591-48-0		0.13		0.04
methylcyclohexane	C7	732	729	108-87-2	0.12	0.48	0.13	0.14
ethylcyclopentane	C7	739	737	1640-89-7	0.04	0.23		0.09
4-methylcyclohexene	C7	742	742	591-47-9		0.28	0.06	0.08
methylenecyclohexane	C7	745	746	1192-37-6		0.16		
2,4-Heptadiene	C7	746	749	628-72-8		0.19		0.06
1-ethylcyclopentene	C7	747	751	2146-38-5		0.22	0.05	0.08
4-methyl-1-heptene	C8	748	755	13151-05-8		0.59	0.1	
4-methyl-2-heptene	C8	751	754	66225-17-0		0.38		0.08
Toluene	Tol	756	759	108-88-3	0.19	1.54	0.51	1.38
4-methylheptane	C8	768	770	589-53-7	0.15	2.3	0.55	0.45
cis-1,3-dimethylcyclohexane	C8	774	772	638-04-0	0.07			
2-methyl-1-heptene	C8	782	784	15870-10-7		0.4	0.07	0.11
3-methyleneheptane 2-Ethyl-1-hexene	C8	785	789	1632-16-2		0.37	0.07	0.15
1-octene	C8	790	798	111-66-0	0.1	2.2	0.57	0.68
octane	C8	800	804	111-65-9	0.32	2.22	0.59	0.69
3-octene	C8	814	814	14919-01-8	0.03	0.21		0.08
2-octene	C8	818	820	13389-42-9		0.14		
3-octyne	C8	820	825	15232-76-5		0.2		
2,4-dimethylheptane	C9	822	828	2213-23-2		0.9	0.2	0.15
(1α,3α,5α)-1,3,5-trimethylcyclohexane	C9	831	832	1795-27-3	0.05	0.81	0.21	0.15
ethylcyclohexane	C8	832	838	1678-91-7	0.17	0.4	0.08	0.1
propylcyclopentane	C8	833	842	1678-92-8	0.09	1.67	0.46	0.32
2,4-dimethyl-1-heptene	C9	842	849	19549-87-2		16.51	4.26	2.74
(1α,3α,5β)-1,3,5-trimethylcyclohexane	C9	850	855	1795-26-2	0.07	1.21	0.4	0.25
ethylbenzene	Etb	857	561	100-41-4	0.12	1.51	0.63	2.1
m-xylene	X	862	869	108-38-3	0.38	0.58	0.34	0.18

Table 2. *Cont.*

Analyte	Analyte Code	RI Lit	RI Calc	CAS	Average % Area MGO (comm)	Average % Area VN (ml-py)	Average % Area MGO (ml-py)	Average % Area RPO (ml-py)
1,8-nonadiene	C9	879	880	4900-30-5		0.25	0.09	0.04
styrene	STY	889	885	100-42-5	0.05	1.11	0.57	2.28
o-xylene	X	891	889	95-47-6	0.12	0.46	0.19	0.16
1-nonene	C9	893	891	124-11-8	0.1	2.05	0.82	0.68
(E)-2-Nonene	C9	897	893	6434-78-2		0.11	0.05	0.05
nonane	C9	900	897	111-84-2	0.72	1.83	0.81	0.67
(Z)-2-Nonene	C9	911	910	6434-77-1		0.27	0.11	0.07
(1-methylethyl)benzene	AR	920	922	98-82-8		0.24	0.14	0.27
propylcyclohexane	C9	923	924	1678-92-8	0.16	0.11	0.06	0.06
butylcyclopentane	C9	936	938	2040-95-1	0.12	0.09	0.05	0.03
2,6-dimethyloctane	C10	937	940	2051-30-1	0.24			
propylbenzene	AR	955	949	103-65-1	0.05	0.12	0.08	0.11
1-ethyl-3-methylbenzene	AR	958	951	620-14-4	0.16	0.16	0.13	0.07
1-ethyl-4-methylbenzene	AR	960	959	622-96-8	0.09	0.1		
4-methylnonane	C10	961	962	17301-94-9	0.22	0.23	0.12	0.07
1,3,5-trimethylbenzene (mesitylene)	AR	964	965	108-67-8		0.26	0.19	0.12
2-methylnonane	C10	965	966	871-83-0	0.36			
3-methylnonane	C10	970	970	5911-04-6	0.29			
1-ethyl-2-methylbenzene	AR	976	972	611-14-3	0.18	0.23	0.15	0.1
alfa methylstyrene	AR	978	975	98-83-9		0.17	0.1	0.41
benzonitrile	BN	982	989	100-47-0		0.18	0.1	0.08
2-methyl-1-nonene	C10	983	990	2980-71-4		0.26	0.12	0.09
1,2,4-trimethylbenzene	AR	987	993	95-63-6	0.37	0.16	0.19	0.12
1-decene	C10	993	998	872-05-9	0.22	2.07	1.37	0.97
decane	C10	1000	1004	124-18-5	1.75	1.45	1.04	0.79
(1-methylpropyl)benzene	AR	1006	1011	135-98-8	0.07			
(Z)-2-decene	C10	1011	1017	20348-51-0		0.24	0.16	0.12
2,5-dimethylnonane	C11	1015	1019	17302-27-1	0.11	0.74	0.51	0.23
2,6-dimethylnonane	C11	1030	1029	17302-28-2	0.2	0.78	0.52	0.27
1,2,3-trimethylbenzene	AR	1032	1032	526-73-8	0.33			
D-limonene	C10	1035	1038	5989-27-5		0.14	0.11	0.22
indane	I	1042	1041	496-11-7	0.12	0.2	0.29	0.3
indene	I	1050	1049	95-13-6		0.15	0.11	0.07
butylbenzene	AR	1055	1058	104-51-8	0.16	0.08	0.09	0.08
5-methyldecane	C11	1056	1060	13151-35-4	0.37	0.35	0.34	0.17
4-methyldecane	C11	1060	1062	2847-72-5	0.35			
2-methyldecane	C11	1063	1065	6975-98-0	0.53			
acetophenone	AcPh	1066	1066	98-86-2		0.19	0.5	0.51
3-methyldecane	C11	1069	1069	13151-34-3	0.41			
2-ethyl-1,4-dimethylbenzene	AR	1074	1074	1758-88-9	0.17		0.07	
1-ethyl-1,2-dimethylbenzene	AR	1082	1078	934-80-5	0.22		0.1	
2-ethyl-1,3-dimethylbenzene	AR	1087	1085	2870-04-4	0.48			
1-undecene	C11	1090	1087	821-95-4	0.15	1.48	1.63	1.08
1-methyl-4-(1-methylpropyl)benzene	AR	1092	1089	1595-16-0	0.24			
undecane	C11	1100	1097	1120-21-4	2.4	1.07	1.25	0.99
(E)-2-Undecene	C11	1104	1110	821-98-7		0.19	0.23	0.14
(Z)-2-undecene	C11	1110	1115	821-96-5		0.15		0.09
decahydro-2-methylnaphthalene (trans-2-methyldecalin)	C11	1115	1117	2958-76-1	0.36			
1,2,4,5-tetramethylbenzene	AR	1116	1118	95-93-2	0.27		0.25	0.09
1,2,3,5-tetramethylbenzene	AR	1119	1120	527-53-7	0.44		0.2	
decahydro-1-methylnaphthalene (1-methyldecalin)	C11	-	1125	2958-75-0	0.31			
3,7-dimethyldecane	C12	1127	1129	17312-54-8	0.31			
pentylcyclohexane	C11	1134	1137	4292-92-6	0.36			
hexylcyclopentane	C11	1136	1139	4457-00-5	0.33			
2,3-dihydro-4-methyl-1H-Indene	I	1147	1150	824-22-6	0.29	0.16	0.26	0.15
pentylbenzene	AR	1155	1152	538-68-1	0.41			
1,2,3,4-tetrahydronaphthalene	N	1162	1161	119-64-2	0.52			
2-methylundecane	C12	1167	1170	7045-71-8	0.73		0.13	0.14
3-methylundecane	C12	1171	1173	1002-43-3	0.42		0.06	0.08
naphthalene	N	1182	1189	91-20-3	0.15	0.18	0.4	0.24
1-dodecene	C12	1193	1190	112-41-4	0.22	0.91	1.59	1.18
dodecane	C12	1200	1205	112-40-3	2.36	0.82	1.46	1.23
(E)-2-dodecene	C12	1201	1208	7206-13-5		0.12	0.21	0.14
(Z)-2-dodecene	C12	1212	1216	7206-16-6		0.07	0.14	0.11
2,6-dimethylundecane	C13	1213	1215	17301-23-4	0.55			
1,2,3,4-tetrahydro-2-methylnaphthalene	N	-	1218	3877-19-8	0.25			
2-butyl-1,1,3-trimethylcyclohexane	C13	1219	1222	54676-39-0	0.36			
2,8-dimethylundecane	C13	1221	1225	17301-25-6		0.11	0.26	0.14
6-methyldodecane	C13	1251	1250	6044-71-9	0.75	0.18	0.42	0.18
hexylbenzene	AR	1255	1253	1077-16-3		0.04	0.18	0.09
4-methyldodecane	C13	1257	1254	6117-97-1	0.29			
2-methyldodecane	C13	1263	1258	1560-97-0	0.68			
1,2,3,4-tetrahydro-5-methylnaphthalene	N	1279	1276	2809-64-5	0.44			

Table 2. *Cont.*

Analyte	Analyte Code	RI Lit	RI Calc	CAS	Average % Area MGO (comm)	Average % Area VN (ml-py)	Average % Area MGO (ml-py)	Average % Area RPO (ml-py)
1-tridecene	C13	1292	1291	2437-56-1	0.41	0.61	1.71	1.28
tridecane	C13	1300	1301	629-50-5	2.65	0.67	1.62	1.65
1-methylnaphthalene	N	1306	1303	90-12-0	0.21	0.32	0.95	0.54
4-methyltridecane	C14	1360	1357	26730-12-1	0.34		0.1	
3-methyltridecane	C14	1369	1370	6418-41-3	0.54		0.07	0.05
2,6,10-trimethyldodecane	C15	1370	1373	3891-98-3	0.32			
biphenyl	BY	1373	1376	92-52-4	0.16	0.12	0.49	0.39
1-tetradecene	C14	1393	1393	1120-36-1	0.52	0.37	1.6	1.26
tetradecane	C14	1400	1402	629-59-4	2.28	0.38	1.6	1.52
(E)-2-tetradecene	C14	1406	1407	35953-53-8		0.09	0.4	0.17
2,6-dimethylnaphthalene	N	1409	1412	581-42-0	0.49			
1,3-dimethylnaphthalene	N	1424	1428	575-41-7	0.36		0.1	0.31
1,5-dimethylnaphthalene	N	1446	1442	571-61-9	0.65			
1,8-dimethylnaphthalene	N	1459	1465	569-41-5	0.21			
3-methyltetradecane	C14	1472	1476	18435-22-8	0.65			
1-pentadecene	C15	1493	1491	13360-61-7	0.56	0.25	1.54	1.47
pentadecane	C15	1500	1507	629-62-9	2.04	0.3	1.67	1.53
2,3,6-trimethylnaphthalene	N	1550	1545	829-26-5	0.37			
1,6,7-trimethylnaphthalene	N	1572	1563	2245-38-7	0.22			
1-hexadecene	C16	1593	1592	629-73-2	0.43	0.15	1.26	1.05
hexadecane	C16	1600	1603	544-76-3	1.47	0.22	1.83	1.55
1,1'-(1,3-propanediyl)bis-benzene	AR	1633	1640	1081-75-0			0.31	0.61
1-heptadecene	C17	1693	1692	6765-39-5	0.28		1.02	0.9
heptadecane	C17	1700	1706	629-78-7	1.26	0.15	1.52	1.42
1-octadecene	C18	1793	1794	112-88-9	0.31	0.06	0.78	1.02
octadecane	C18	1800	1806	593-45-3	1.09	0.11	1.29	1.24
1-nonadecene	C19	1893	1893	18435-45-5	0.43	0.03	0.63	1.24
nonadecane	C19	1900	1902	629-92-5	1.06	0.08	1.11	1.41
1-eicosene	C20	1993	1992	3452-07-1	0.16		0.43	0.54
eicosane	C20	2000	1999	112-95-8	1.05	0.06	1.2	1.53
1-heneicosene	C21	2093	2093	27400-79-9	0.15		0.26	0.34
heneicosane	C21	2100	2104	629-94-7	0.9	0.03	0.76	1.2
pyrene	PHA	2126	2128	129-00-0	0.17		0.07	
1-docosene	C22	2193	2193	1599-67-3	0.09		0.19	0.41
docosane	C22	2200	2202	629-97-0	0.6	0.02	0.55	0.94
1-tricosene	C23	2293	2295		0.07		0.12	0.15
tricosane	C23	2300	2301	638-67-5	0.49		0.39	0.69
tetracosane	C24	2400	2404	646-31-1	0.32		0.53	0.7
pentacosane	C25	2500	2503	629-99-2	0.24		0.3	0.4
hexacosane	C26	2600	2601	630-01-3	0.13		0.29	0.34
heptacosane	C27	2700	2702				0.19	0.14
Octacosane	C28	2800	2800	630-02-4			0.19	0.13

For MGO (comm), VN (ml-py), MGO (ml-py), and RPO (ml-py), 120, 117, 120, and 131 compounds were identified, respectively, and they represent 34%, 43%, 38%, and 32% of the detected compounds, respectively.

Figure 2 details the cumulative average percent area of the identified compounds. Noteworthy, the BTX, ethylbenzene, styrene, and alpha-methylstyrene contents in VN (ml-py) are ca. twofold compared to MGO (ml-py). This is important because they are potentially recoverable platform chemicals for industrial application. BTX separation from petroleum naphtha is state-of-the-art technology, and it is generally performed by liquid–liquid extraction with sulfolane [43,44]. Removing BTX from VN (ml-py) would attain a double result: obtaining valuable aromatics for the chemical industry and aromatic-free naphtha, the ideal feedstock for the steam cracking process and the synthesis of polyolefins, and hence, new virgin PE and PP polymers [43]. Besides, building blocks from the pyrolysis are often the monomers of the processed polymers (e.g., styrene) that can be subsequently polymerized again [3]. This latter development is a work in progress at present. Similarly, the content of light aliphatic compounds ranging between C5 and C11 is higher in VN (ml-py) compared to MGO (ml-py); in particular, the contents of the C5–C7 compounds and the C8–C9 compounds in VN (ml-py) are at least fivefold and threefold, respectively, compared to MGO (ml-py). In VN (ml-py), aliphatic compounds with a number of carbon atoms higher than 22 were not detected. On the contrary, the content of aliphatic compounds ranging between C12 and C28 is higher in MGO (ml-py) compared to VN (ml-py), as expected. Many specific compounds detailed in Table 2 were already found in pyrolysis oils from specific plastic materials or mixed plastic waste. The general aspects of the pyrolytic degradation mechanism of polymers involve three kinds of chain reactions viz. polymeric chain scissions, side group reactions, and recombination

reactions. For example, the thermal degradation of both HDPE and PP yielded alkanes, alkenes, and alkynes; double-bonded hydrocarbons compounds are generated via the single-bonded carbon (C–C) dissociation in a polyalkane structure and the stabilization of free radicals produced from the chain scissoring mechanism [29]. From the data in Table 2, it is clear that olefins (alkenes, cycloalkenes, and polyenes) constitute a very important family of pyrolysis compounds, comprising 40.45%, 23.23%, and 22.08% of the area of VN (ml-py), MGO (ml-py), and RPO (ml-py) samples, respectively; it follows that VN (ml-py) might be an interesting source of these precious building blocks for the chemical industry. Linear alpha olefins (normal alpha olefins) from 1-hexene to 1-tridecene were typical of HDPE pyrolysis, and 1-heptene and 1-octene were also found to be markers of the PP pyrolysis [11]. We found these compounds to be very expedient in the chemical industry. They are lighter in terms of the homologous series of the linear alpha olefins up to 1-octene and are used (i) as a comonomer in the production of polyethylene and (ii) as feedstock for the hydroformylation process to produce linear aldehyde via oxo synthesis and, subsequently, short-chain fatty acids (via aldehyde oxidation) or linear alcohols (via aldehyde hydrogenation) for plasticizer applications. Abundant amounts of C10-C13 linear alpha olefins can be upcycled in making surfactants: their reaction with benzene generates linear alkylbenzenes (LAB), and their subsequent sulfonation yields linear alkylbenzene sulfonates (LABS), which is a popular low-cost surfactant for household and industrial detergent applications. Alkynes were seldomly identified. Alkanes and cycloalkanes constantly represent ca. 25% of the eluted area for all samples. PP methyl side groups were reported to increase the yield of branched hydrocarbons and alkenes compared to PE [29,45]. Actually, we found, as detailed in Table 2, 2-methyl-1-pentene, 2,4-dimethyl-1-heptene, and 3-methylcyclopentene related to PP, as well as trimethyl cyclohexanes [11,29] and many other branched hydrocarbons and alkenes. The largest eluted percent area in the VN (ml-py), MGO (ml-py), and RPO (ml-py) samples is constantly due to 2,4-dimethyl-1-heptene, which represents 16.51%, 4.26%, and 2.74% of the area, respectively. A major source of aromatic building blocks in the pyrolysis oil is PS breakdown, which involves the elimination of styrene moieties thereby increasing the number of aromatic compounds in pyrolysis oil; in addition, PET is a contributor as it is reported that PET pyrolysis leads to a benzene-rich pyrolysis oil, in particular, high temperatures and slow heating rates maximize the amount of aromatics and the selectivity of benzene [46]. However, in this work, pyrolysis was performed in the presence of calcium-based additives, and PET decomposes into terephthalic and benzoic acids at 350 °C, which are subsequently decarboxylated into aromatics thanks to CaO. Kumagai et al. reported an increase in benzene yield when terephthalic acid is decarboxylated in the presence of CaO [47,48].

As regards aromatics identified and detailed in Table 2, benzene, toluene, and xylenes may come from multiple plastic waste sources (HDPE, LDPE, PP, PS, and PET), while ethylbenzene was related to PP and PS pyrolysis; styrene, propyl benzene, and 1-ethyl-2-methylbenzene were particularly reported to be markers of PS pyrolysis [11]. Even if [13] it was reported that no aromatic groups were identified in the pyrolysis oil from virgin PP and HDPE, it is well known that aromatics are generated during PP pyrolysis from secondary reactions via cyclization and aromatization reactions, especially at high processing temperatures and heating rates [12]; the low molecular weight olefins (C2–C5) from PE and PP may undergo the Diels–Alder intermolecular cyclization and radical intramolecular cyclization. A subsequent dehydrogenation process rationalizes the formation of aromatic compounds [49–52]. Furthermore, the interactions of different plastic wastes during the pyrolysis process were reported to increase the content of aromatic compounds [53–56]. In Table 2, the presence of trimethylbenzenes, indane, and indene can be related to LDPE pyrolysis, even if indene was also related to PP [11]. Naphthalene is generated by the LDPE and PS pyrolysis, while 1-methylnaphthalene, dimethyl naphthalenes, and trimethyl naphthalenes are markers of PVC and LDPE pyrolysis. Biphenyl was related to PET, PVC, and PP pyrolysis feedstocks [11]. Oxygen and nitrogen compounds were previously reported to be a residual fraction in pyrolysis oil samples [3,13,27,57]; actually, only benzonitrile was

identified (both in distillates and in the RPO). The lack of oxygenated compounds among those identified in Table 2 is expedient since high oxygen content results in low calorific value, corrosion problems, and instability; the presence of PS can drastically abate the oxygen content, thereby mimicking the diesel standard [57]. Some putative sulfur, nitrogen, and oxygen compounds were detected but not positively identified.
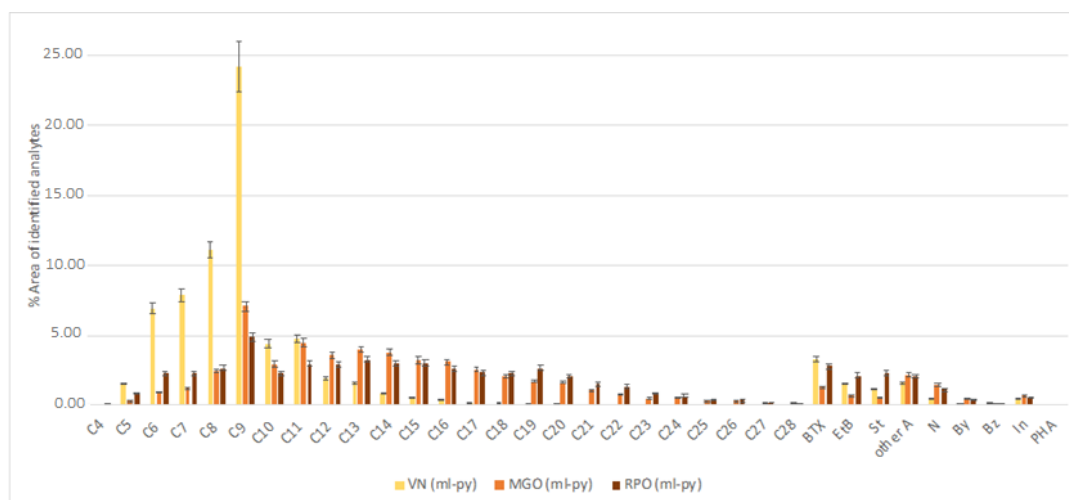

Figure 2. Averaged percent area and standard deviations (triplicate injections of the identified compounds, grouped as indicated in the abscissa for VN (ml-py), MGO (ml-py), and RPO (ml-py) samples. C4-C28: aliphatic hydrocarbons with 4 to 28 carbon atoms; BTX: benzene + toluene + xylenes; EtB: ethylbenzene; St: styrene; other A: other monoaromatics; N: naphthenic compounds; By: biphenyl; Bz; benzonitrile; In: indane and indene compounds; PHA: Pyrene.

The top three compounds in the eluted area for the VN (ml-py) are 2,4-dimethyl-1-heptene (16.51%), 1-hexene (2.87%), and 4-methylheptane (2.30%) followed by short-chain alpha-olefins. Those for MGO (ml-py) are 2,4-dimethyl-1-heptene (4.26%), hexadecane (1.83%), and 1-tridecene (1.71%), followed by linear alkanes and alpha-olefins. For RPO (ml-py) we have 2,4-dimethyl-1-heptene (2.74%), styrene (2.28%), and ethylbenzene (2.1%), mainly followed by linear alkanes with a carbon number higher than 13. For MGO (comm), the most represented compounds are tridecane (2.65%), undecane (2.40%), and dodecane (2.36%), followed by linear alkanes with a carbon number higher than 10. It can be confirmed that 2,4-dimethyl-1-heptene, detected in all samples obtained from the pyrolysis but in MGO (comm), is a good putative marker of the plastic origin of the fuel.

From Figure 3 it is clear that the olefin content is significantly higher in samples from pyrolysis, while paraffins are characteristic of MGO (comm). VN is the richest sample as regards olefins.

In an attempt to go more in depth with the comparison and to confirm or disconfirm similarities, Figure 4 illustrates the averaged percent area of identified analyte in MGO (comm) and MGO (ml-py). The presence of massive amounts of 2,4-dimethyl-1-heptene in the MGO from marine litter pyrolysis oil (ml-py), due to the PP presence [43], differentiate the GC-MS fingerprints of these samples. The presence of naphthalenes is stronger in commercial MGO, compared to its pyrolysis analog. Notwithstanding this, MGO (ml-py) is compliant with ISO8217 specifications as regards marine gasoil, and the incomplete overlap between the molecular fingerprints of MGO (comm) and MGO (ml-py), as evident from Table 2, does not underscore an a priori better or worse performance of the fuel based on marine litter. Further testing of MGO (ml-py) as regards emissions and other parameters is a work in progress since pyrolyzed oil-based fuels could lead to reduced emissions [9,19].
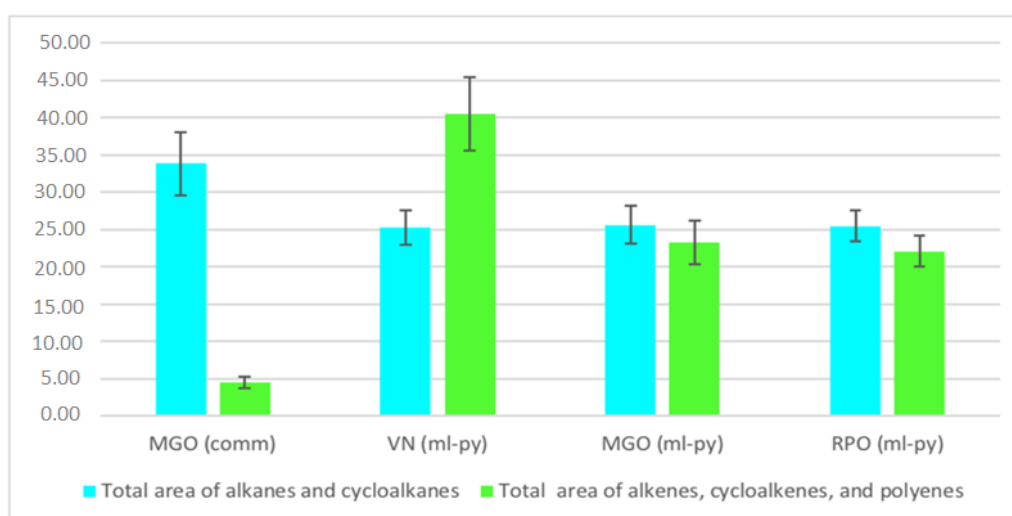
Figure 3. Total area of alkanes and cycloalkanes (light blue) and total area of alkenes, cycloalkenes, and polyenes (green) with standard deviations (triplicate injections) from the GC-MS analysis of MGO (comm), VN (ml-py), MGO (ml-py), and RPO (ml-py).
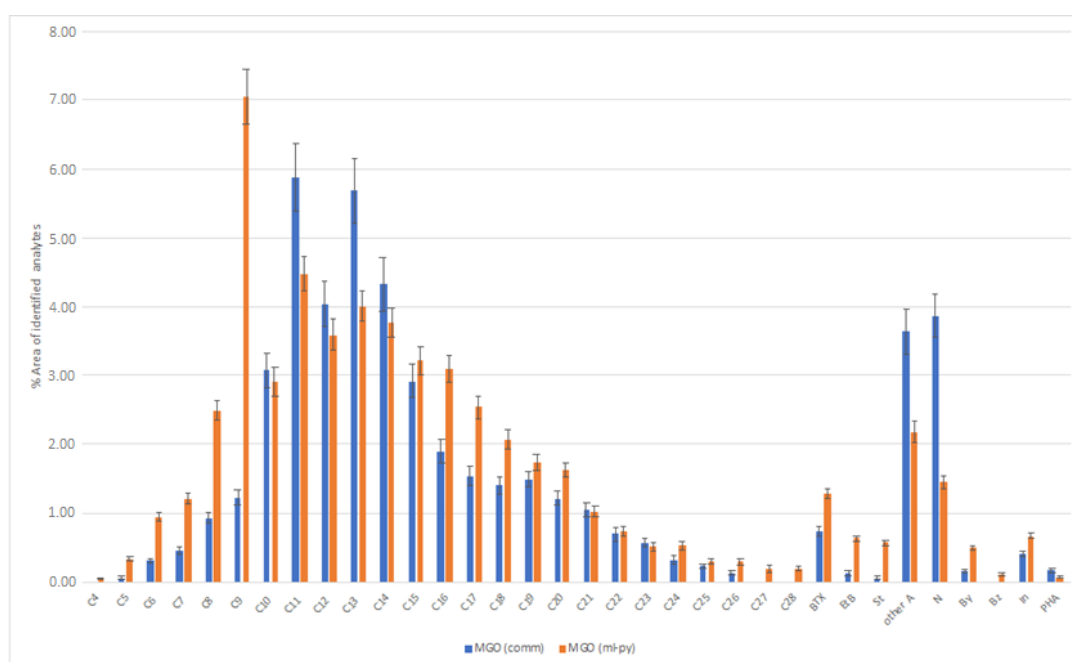

Figure 4. Averaged percent area and standard deviations (triplicate injections) of the identified analyte in MGO (comm) and MGO (ml-py).

Since Figure 3 takes into account only identified compounds, we decided to compare the chromatographic fingerprints of these samples displaying the total percent of the eluted area as a function of time, as shown in Figure 5, in order to avoid artefacts due to the lack of identification of some analytes. The overlap between the two series is impressive, even if we know that saturated hydrocarbons are more common in MGO (comm), and unsaturated compounds are more common in MGO (ml-py). Again, for the MGO (ml-py) series, the massive presence of 2,4-dimethyl-1-heptene and 1-nonene eluted at 16 and 20minutes, respectively, explains the appearance of two putative outliers. The majority of the eluted area resides between 28 min and 44 min, corresponding, to an oven temperature of 95 °C and 250 °C, respectively.
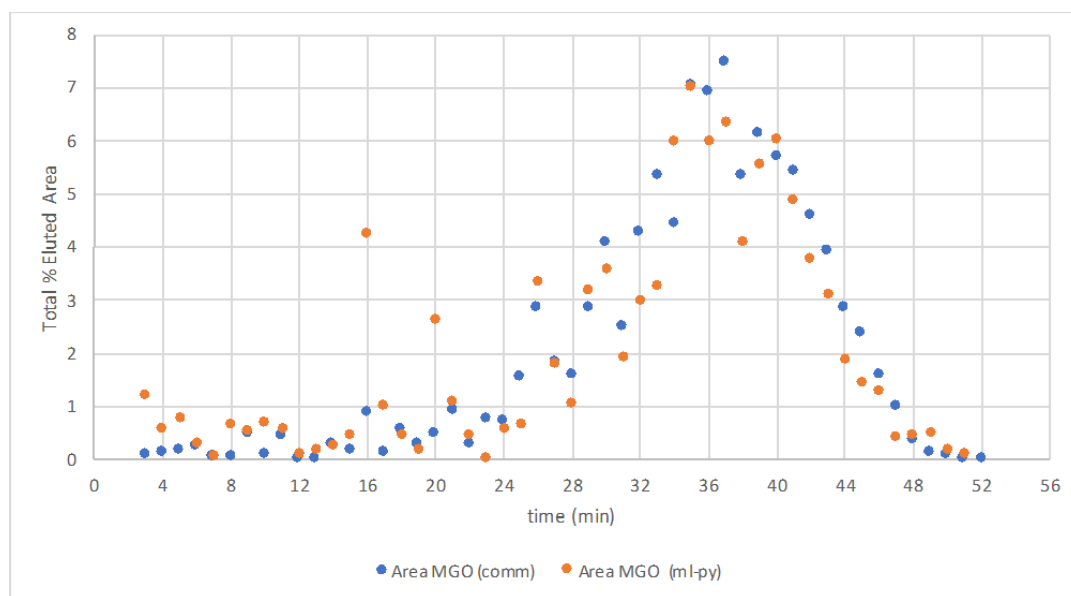
Figure 5. Total averaged percent of the eluted area as a function of the chromatographic time for MGO (comm) and MGO (ml-py) samples.

3.3. FTIR Analysis

Pyrolysis oil, its distillates, and commercial MGO are complex mixtures of alkanes, alkenes, aromatic and other compounds hence their FTIR spectra are complicated. FTIR analysis in a wave range of 4000–600 cm^{-1} using an ATR arrangement can highlight the presence of functional groups but also provide a chemical signature of the samples [11]. The spectra are shown in Figure 6.
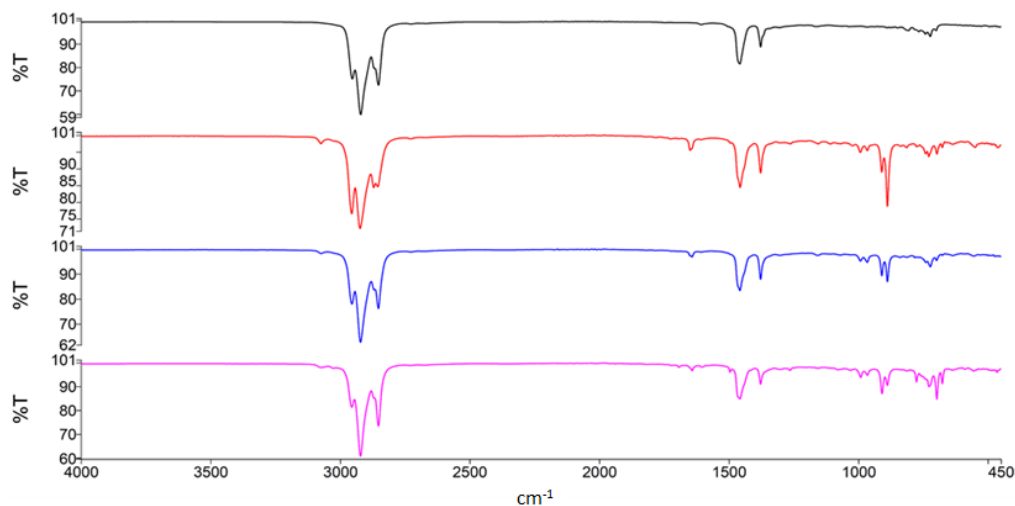
Figure 6. FTIR spectra of MGO (comm) (black curve); VN (ml-py) (red curve); MGO (ml-py) (blue curve); and RPO (ml-py) (pink curve).

For the most part, the spectra can be classified into 3 wavenumber ranges based on the absorption bands observed ranging between 3100 cm^{-1} and 2800 cm^{-1}, 1700 cm^{-1} and 1300 cm^{-1}, and 1000 cm^{-1} and 600 cm^{-1}. They all represent typical hydrocarbon vibrations. In all samples, the absorption bands between 3000 cm^{-1} and 2800 cm^{-1} at wave number 2923–2925 cm^{-1} and 2854–2856 cm^{-1} represent the aliphatic asymmetric (υasC—-H) and symmetric (υsC——H) stretching vibrations of the –CH2 group. The absorption bands at wave number 2955–2957 cm^{-1} and 2872cm^{-1} represent the aliphatic

asymmetric (υasC—-H) and symmetric (υsC—-H) stretching vibrations of the –CH3 group. While the former is present in all samples, the latter is clearly visible only in the VN (ml-py) sample. The set of two peaks at 1457 cm^{-1} and 1377 cm^{-1} highlight the sp3 C–H asymmetric and symmetric bending [58].

The band at 722 cm^{-1} is due to the rocking of the –CH2– groups and the intensity of this band increases with increasing carbon chain [59]; actually, the strongest band is observed in RPO (ml-py). The massive presence of olefins in the pyrolysis sample is confirmed by their FTIR spectra. In all samples from marine litter pyrolysis, a variance with MGO (comm) the small adsorption band at 3075 cm^{-1} indicates alkene C–H stretching. The band at 1650 cm^{-1} representing the alkene C–C bond stretching confirms the higher presence of olefins [60] in the pyrolysis samples, consistent with results shown in Figure 3. This band is not detectable in MGO (comm), since, as also indicated in Figure 3, in this sample, olefins are less represented. The two strong absorption bands at 990–992 cm^{-1} and 908–909 cm^{-1} represent the C–H stretching of the monosubstituted double bond, and it is missing only in MGO (comm); the peak at 887–888 cm^{-1} marks the presence of a vinylidene-type double bond only in all samples from marine litter pyrolysis. The peak at 697–675 cm^{-1} reinforced the identification of the alkene =C–H bending vibration. The presence of the aromatic group can be inferred from the presence of the C–H stretching between 3100 cm^{-1} and 3000 cm^{-1} and the small C=C stretching aromatic bands at 1495 cm^{-1} [57] that are absent in MGO (comm).

Overall, the spectra obtained are in good agreement with the published literature for pyrolysis oil from mixed plastic waste [29,57,58,60].

4. Conclusions

Recycling difficult plastic waste streams is crucial for a successful circular economy and to reduce environmental pollution. This goal can be achieved through chemical recycling using pyrolysis and distillation. Following this route, plastic marine litter collected from the sea bottom of the northern Adriatic Sea was processed "as it is" and converted into useful ISO-compliant marine gasoil and useful material for the chemical industry. Since marine litter is probably the most difficult waste to upcycle, the same approach could be applied to all kinds of rejected plastic waste and highly nonhomogeneous plastic streams, which do not find a proper recycling solution. Compliance of waste-derived MGO (ml-pl) with ISO8217 standards is demonstrated, and its chemical composition is finally revealed, which is different from the one of conventional MGO (comm). In particular, the presence of massive amounts of 2,4-dimethyl-1-heptene can be considered the chemical signature of plastic-derived fuels and might be used as tracer for its presence for commercialization and blending. A significant amount of valuable aromatics (BTX) then alkenes, cycloalkenes, and polyenes suggest that VN (ml-py) might be an interesting source of these precious building blocks for the chemical industry and even be used as alternative feedstock for the production of virgin polymers using state-of-the-art technologies. A future outlook will be the use of distillates derived from marine litter in steam cracking equipment for the manifacturing of ethilene and propylene to be polymerized into virgin PE and PP.

Author Contributions: Conceptualization, G.C.F. and T.C.; methodology, G.C.F. and T.C.; investigation G.C.F. and T.C.; writing, G.C.F. and T.C.; visualization, G.C.F. and T.C..; supervision, G.C.F.; project administration, G.C.F.; funding acquisition, G.C.F. All authors have read and agreed to the published version of the manuscript.

Data Availability Statement: The data are contained within the article.

Conflicts of Interest: The authors declare no conflict of interest.

Abbreviations

MGO (comm)	commercial marine gasoil
VN (ml-py)	virgin naphtha from marine litter pyrolysis
MGO (ml-py)	marine gasoil from marine litter pyrolysis
RPO (ml-py)	raw oil from marine litter pyrolysis
GC-MS	Gas Chromatography-Mass Spectrometry

References

1. Wayman, C.; Niemann, H. The fate of plastic in the ocean environment—A minireview. *Environ. Sci. Process. Impacts* **2021**, *23*, 198–212. [CrossRef]
2. Canning-Clode, J.; Sepúlveda, P.; Almeida, S.; Monteiro, J. Will COVID-19 Containment and Treatment Measures Drive Shifts in Marine Litter Pollution? *Front. Mar. Sci.* **2020**, *7*. [CrossRef]
3. Baena-González, J.; Santamaria-Echart, A.; Aguirre, J.L.; González, S. Chemical recycling of plastic waste: Bitumen, solvents, and polystyrene from pyrolysis oil. *Waste Manag.* **2020**, *118*, 139–149. [CrossRef]
4. Ragaert, K.; Delva, L.; Van Geem, K. Mechanical and chemical recycling of solid plastic waste. *Waste Manag.* **2017**, *69*, 24–58. [CrossRef] [PubMed]
5. Iñiguez-Cantos, M.E.; Conesa, J.; Fullana, A. Marine debris occurrence and treatment: A review. *Renew. Sustain. Energy Rev.* **2016**, *64*, 394–402. [CrossRef]
6. Aguado, J.; Serrano, D.P.; Escola, J.M. Catalytic Upgrading of Plastic Wastes. In *Feedstock Recycling and Pyrolysis of Waste Plastics: Converting Waste Plastics into Diesel and Other Fuels*; Royal Society of Chemistry: London, UK, 2006; pp. 73–110. [CrossRef]
7. Toraman, H.E.; Dijkmans, T.; Djokic, M.R.; Van Geem, K.M.; Marin, G.B. Detailed compositional characterization of plastic waste pyrolysis oil by comprehensive two-dimensional gas-chromatography coupled to multiple detectors. *J. Chromatogr. A* **2014**, *1359*, 237–246, Erratum in *Arab. J. Geosci.* **2020**, *13*, 504. [CrossRef]
8. Larrain, M.; Van Passel, S.; Thomassen, G.; Kresovic, U.; Alderweireldt, N.; Moerman, E.; Billen, P. Economic performance of pyrolysis of mixed plastic waste: Open-loop versus closed-loop recycling. *J. Clean. Prod.* **2020**, *270*, 122442. [CrossRef]
9. Tomar, M.; Jain, A.; Pujari, P.C.; Dewal, H.; Kumar, N. Potentials of waste plastic pyrolysis oil as an extender fuel for diesel engine. *Arab. J. Geosci.* **2020**, *13*, 1–10. [CrossRef]
10. Papari, S.; Bamdad, H.; Berruti, F. Pyrolytic Conversion of Plastic Waste to Value-Added Products and Fuels: A Review. *Materials* **2021**, *14*, 2586. [CrossRef]
11. Anuar Sharuddin, S.D.; Abnisa, F.; Wan Daud, W.M.A.; Aroua, M.K. A review on pyrolysis of plastic wastes. *Energy Convers. Manag.* **2016**, *115*, 308–326. [CrossRef]
12. Abbas-Abadi, M.S.; Nekoomanesh-Haghighi, M.; Yeganeh, H.; McDonald, A.G. Evaluation of pyrolysis process parameters on polypropylene degradation products. *J. Anal. Appl. Pyrolysis* **2014**, *109*, 272–277. [CrossRef]
13. Ahmad, I.; Khan, M.I.; Khan, H.; Ishaq, M.; Tariq, R.; Gul, K.; Ahmad, W. Pyrolysis Study of Polypropylene and Polyethylene Into Premium Oil Products. *Int. J. Green Energy* **2014**, *12*, 663–671. [CrossRef]
14. López, A.; de Marco, I.; Caballero, B.; Laresgoiti, M.; Adrados, A. Pyrolysis of municipal plastic wastes: Influence of raw material composition. *Waste Manag.* **2010**, *30*, 620–627. [CrossRef]
15. Onwudili, J.; Insura, N.; Williams, P. Composition of products from the pyrolysis of polyethylene and polystyrene in a closed batch reactor: Effects of temperature and residence time. *J. Anal. Appl. Pyrolysis* **2009**, *86*, 293–303. [CrossRef]
16. Amjad, U.; Ishaq, M.; Rehman, H.U.; Ahmad, N.; Sherin, L.; Hussain, M.; Mustafa, M. Diesel and gasoline like fuel production with minimum styrene content from catalytic pyrolysis of polystyrene. *Environ. Prog. Sustain. Energy* **2020**, *40*, e13493. [CrossRef]
17. Sogancioglu, M.; Yel, E.; Ahmetli, G. Investigation of the Effect of Polystyrene (PS) Waste Washing Process and Pyrolysis Temperature on (PS) Pyrolysis Product Quality. *Energy Procedia* **2017**, *118*, 189–194. [CrossRef]
18. Rehan, M.; Miandad, R.; Barakat, M.A.; Ismail, I.M.I.; Almeelbi, T.; Gardy, J.; Hassanpour, A.; Khan, M.Z.; Demirbas, A.; Nizami, A.S. Effect of zeolite catalysts on pyrolysis liquid oil. *Int. Biodeterior. Biodegrad.* **2017**, *119*, 162–175. [CrossRef]
19. Mangesh, V.L.; Padmanabhan, S.; Tamizhdurai, P.; Ramesh, A. Experimental investigation to identify the type of waste plastic pyrolysis oil suitable for conversion to diesel engine fuel. *J. Clean. Prod.* **2020**, *246*, 119066. [CrossRef]
20. Gaurh, P.; Pramanik, H. Production of benzene/toluene/ethyl benzene/xylene (BTEX) via multiphase catalytic pyrolysis of hazardous waste polyethylene using low cost fly ash synthesized natural catalyst. *Waste Manag.* **2018**, *77*, 114–130. [CrossRef] [PubMed]
21. Gaurh, P.; Pramanik, H. A novel approach of solid waste management via aromatization using multiphase catalytic pyrolysis of waste polyethylene. *Waste Manag.* **2018**, *71*, 86–96. [CrossRef]
22. Venkatesan, H.; Sivamani, S.; Bhutoria, K.; Vora, H.H. Assessment of waste plastic oil blends on performance, combustion and emission parameters in direct injection compression ignition engine. *Int. J. Ambient Energy* **2019**, *40*, 170–178. [CrossRef]

23. Areeprasert, C.; Asingsamanunt, J.; Srisawat, S.; Kaharn, J.; Inseemeesak, B.; Phasee, P.; Khaobang, C.; Siwakosit, W.; Chiemchaisri, C. Municipal Plastic Waste Composition Study at Transfer Station of Bangkok and Possibility of its Energy Recovery by Pyrolysis. *Energy Procedia* **2017**, *107*, 222–226. [CrossRef]

24. Sarker, M.; Rashid, M.M.; Molla, M. Waste polypropylene plastic conversion into liquid hydrocarbon fuel for producing electricity and energies. *Environ. Technol.* **2012**, *33*, 2709–2721. [CrossRef]

25. Yan, G.; Jing, X.; Wen, H.; Xiang, S. Thermal Cracking of Virgin and Waste Plastics of PP and LDPE in a Semibatch Reactor under Atmospheric Pressure. *Energy Fuels* **2015**, *29*, 2289–2298. [CrossRef]

26. Huang, W.-C.; Huang, M.-S.; Huang, C.-F.; Chen, C.-C.; Ou, K.-L. Thermochemical conversion of polymer wastes into hydrocarbon fuels over various fluidizing cracking catalysts. *Fuel* **2010**, *89*, 2305–2316. [CrossRef]

27. Cho, M.-H.; Jung, S.-H.; Kim, J.-S. Pyrolysis of Mixed Plastic Wastes for the Recovery of Benzene, Toluene, and Xylene (BTX) Aromatics in a Fluidized Bed and Chlorine Removal by Applying Various Additives. *Energy Fuels* **2010**, *24*, 1389–1395. [CrossRef]

28. Ateş, F.; Miskolczi, N.; Borsodi, N. Comparision of real waste (MSW and MPW) pyrolysis in batch reactor over different catalysts. Part I: Product yields, gas and pyrolysis oil properties. *Bioresour. Technol.* **2013**, *133*, 443–454. [CrossRef]

29. Singh, R.K.; Ruj, B.; Sadhukhan, A.K.; Gupta, P. Thermal degradation of waste plastics under non-sweeping atmosphere: Part 2: Effect of process temperature on product characteristics and their future applications. *J. Environ. Manag.* **2020**, *261*, 110112. [CrossRef]

30. Allison, E.H.; Cheung, W.W.L.; Dey, M.M.; Halpern, B.S.; Mccauley, D.J.; Smith, M.; Vaitla, B.; Zeller, D.; Myers, S.S.; Nilsson, M.; et al. The State of World Fisheries and Aquaculture (SOFIA) 2010. *FAO Proc. Nat. Acad. Sci.* **2013**, *382*.

31. Galgani, F.; Hanke, G.; Maes, T. Global Distribution, Composition and Abundance of Marine Litter. In *Marine Anthropogenic Litter*; Springer: Cham, Switzerland, 2015; pp. 29–56. [CrossRef]

32. Consoli, P.; Falautano, M.; Sinopoli, M.; Perzia, P.; Canese, S.; Esposito, V.; Battaglia, P.; Romeo, T.; Andaloro, F.; Galgani, F.; et al. Composition and abundance of benthic marine litter in a coastal area of the central Mediterranean Sea. *Mar. Pollut. Bull.* **2018**, *136*, 243–247. [CrossRef]

33. PlasticsEurope. *The Facts 2018*; PlasticsEurope: Brussels, Belgium, 2018.

34. Okuwaki, A.; Yoshioka, T.; Asai, M.; Tachibana, H.; Wakai, K.; Tada, K. The Liquefaction of Plastic Containers and Packaging in Japan. In *Feedstock Recycling and Pyrolysis of Waste Plastics: Converting Waste Plastics into Diesel and Other Fuels*; John Wiley & Sons: Hoboken, NJ, USA, 2006; pp. 663–708. [CrossRef]

35. Ripari, V.; Tomassetti, M.; Cecchi, T.; Enrico, B. Recipe, volatiles profile, sensory analysis, physico-chemical and microbial characterization of acidic beers from both sourdough yeasts and lactic acid bacteria. *Eur. Food Res. Technol.* **2018**, *244*, 2027–2040. [CrossRef]

36. Ripari, V.; Cecchi, T.; Berardi, E. Microbiological characterisation and volatiles profile of model, ex-novo, and traditional Italian white wheat sourdoughs. *Food Chem.* **2016**, *205*, 297–307. [CrossRef] [PubMed]

37. Benucci, I.; Cecchi, T.; Lombardelli, C.; Maresca, D.; Mauriello, G.; Esti, M. Novel microencapsulated yeast for the primary fermentation of green beer: Kinetic behavior, volatiles and sensory profile. *Food Chem.* **2020**, *340*, 127900. [CrossRef]

38. Cecchi, T.; Alfei, B. Volatile profiles of Italian monovarietal extra virgin olive oils via HS-SPME–GC–MS: Newly identified compounds, flavors molecular markers, and terpenic profile. *Food Chem.* **2013**, *141*, 2025–2035. [CrossRef]

39. Cherfaoui, M.; Cecchi, T.; Keciri, S.; Boudriche, L. Volatile compounds of Algerian extra-virgin olive oils: Effects of cultivar and ripening stage. *Int. J. Food Prop.* **2018**, *21*, 36–49. [CrossRef]

40. Madricardo, F.; Ghezzo, M.; Nesto, N.; Mc Kiver, W.J.; Faussone, G.C.; Fiorin, R.; Riccato, F.; Mackelworth, P.C.; Basta, J.; De Pascalis, F.; et al. How to Deal With Seafloor Marine Litter: An Overview of the State-of-the-Art and Future Perspectives. *Front. Mar. Sci.* **2020**, *7*, 830. [CrossRef]

41. Faussone, G.C.; Kržan, A.; Grilc, M. Conversion of Marine Litter from Venice Lagoon into Marine Fuels via Thermochemical Route: The Overview of Products, Their Yield, Quality and Environmental Impact. *Sustainability* **2021**, *13*, 9481. [CrossRef]

42. IMO Annex 14, Resolution MEPC. 320(74) (adopted 17 May2019). 2019 Guidelines for Consistent Implementation ofthe 0.50% Sulphur Limit Under Marpol Annex VI. Available online: https://wwwcdn.imo.org/localresources/en/OurWork/Environment/Documents/Resolution%20MEPC.320%2874%29.pdf. (accessed on 1 November 2021).

43. Choi, Y.J.; Cho, K.W.; Cho, B.W.; Yeo, Y.-K. Optimization of the Sulfolane Extraction Plant Based on Modeling and Simulation. *Ind. Eng. Chem. Res.* **2002**, *41*, 5504–5509. [CrossRef]

44. Bak, A.; Kozik, V.; Dybal, P.; Kus, S.; Swietlicka, A.; Jampilek, J. Sulfolane: Magic Extractor or Bad Actor? Pilot-Scale Study on Solvent Corrosion Potential. *Sustainability* **2018**, *10*, 3677. [CrossRef]

45. Pinto, F.; Costa, P.; Gulyurtlu, I.; Cabrita, I. Pyrolysis of plastic wastes. 1. Effect of plastic waste composition on product yield. *J. Anal. Appl. Pyrolysis* **1999**, *51*, 39–55. [CrossRef]

46. Du, S.; Valla, J.A.; Parnas, R.S.; Bollas, G.M. Conversion of Polyethylene Terephthalate Based Waste Carpet to Benzene-Rich Oils through Thermal, Catalytic, and Catalytic Steam Pyrolysis. *ACS Sustain. Chem. Eng.* **2016**, *4*, 2852–2860. [CrossRef]

47. Kumagai, S.; Grause, G.; Kameda, T.; Takano, T.; Horiuchi, H.; Yoshioka, T. Decomposition of Gaseous Terephthalic Acid in the Presence of CaO. *Ind. Eng. Chem. Res.* **2011**, *50*, 1831–1836. [CrossRef]

48. Kumagai, S.; Grause, G.; Kameda, T.; Takano, T.; Horiuchi, H.; Yoshioka, T. Improvement of the Benzene Yield During Pyrolysis of Terephthalic Acid Using a CaO Fixed-Bed Reactor. *Ind. Eng. Chem. Res.* **2011**, *50*, 6594–6600. [CrossRef]

49. Abbas-Abadi, M.S. The effect of process and structural parameters on the stability, thermo-mechanical and thermal degradation of polymers with hydrocarbon skeleton containing PE, PP, PS, PVC, NR, PBR and SBR. *J. Therm. Anal.* **2021**, *143*, 2867–2882. [CrossRef]

50. Jin, Z.; Chen, D.; Yin, L.; Hu, Y.; Zhu, H.; Hong, L. Molten waste plastic pyrolysis in a vertical falling film reactor and the influence of temperature on the pyrolysis products. *Chin. J. Chem. Eng.* **2018**, *26*, 400–406. [CrossRef]

51. Liu, X.; Li, X.; Liu, J.; Wang, Z.; Kong, B.; Gong, X.; Yang, X.; Lin, W.; Guo, L. Study of high density polyethylene (HDPE) pyrolysis with reactive molecular dynamics. *Polym. Degrad. Stab.* **2014**, *104*, 62–70. [CrossRef]

52. Park, K.-B.; Jeong, Y.-S.; Guzelciftci, B.; Kim, J.-S. Characteristics of a new type continuous two-stage pyrolysis of waste polyethylene. *Energy* **2018**, *166*, 343–351. [CrossRef]

53. Muhammad, C.; Onwudili, J.A.; Williams, P.T. Thermal Degradation of Real-World Waste Plastics and Simulated Mixed Plastics in a Two-Stage Pyrolysis–Catalysis Reactor for Fuel Production. *Energy Fuels* **2015**, *29*, 2601–2609. [CrossRef]

54. Miandad, R.; Barakat, M.; Aburiazaiza, A.S.; Rehan, M.; Nizami, A. Catalytic pyrolysis of plastic waste: A review. *Process Saf. Environ. Prot.* **2016**, *102*, 822–838. [CrossRef]

55. Miandad, R.; Barakat, M.; Aburiazaiza, A.S.; Rehan, M.; Ismail, I.; Nizami, A. Effect of plastic waste types on pyrolysis liquid oil. *Int. Biodeterior. Biodegrad.* **2017**, *119*, 239–252. [CrossRef]

56. Williams, P.; Slaney, E. Analysis of products from the pyrolysis and liquefaction of single plastics and waste plastic mixtures. *Resour. Conserv. Recycl.* **2007**, *51*, 754–769. [CrossRef]

57. Sharuddin, S.D.A.; Abnisa, F.; Daud, W.M.A.W.; Aroua, M.K. Energy recovery from pyrolysis of plastic waste: Study on non-recycled plastics (NRP) data as the real measure of plastic waste. *Energy Convers. Manag.* **2017**, *148*, 925–934. [CrossRef]

58. Das, P.; Tiwari, P. Valorization of packaging plastic waste by slow pyrolysis. *Resour. Conserv. Recycl.* **2018**, *128*, 69–77. [CrossRef]

59. Miskolczi, N.; Angyal, A.; Bartha, L.; Valkai, I. Fuels by pyrolysis of waste plastics from agricultural and packaging sectors in a pilot scale reactor. *Fuel Process. Technol.* **2009**, *90*, 1032–1040. [CrossRef]

60. Williams, E.A.; Williams, P.T. The pyrolysis of individual plastics and a plastic mixture in a fixed bed reactor. *J. Chem. Technol. Biotechnol.* **1997**, *70*, 9–20. [CrossRef]